Research Article

Fueangfakan Chutrakulwong and Kheamrutai Thamaphat*

Green synthesis of silver nanoparticles using durian rind extract and optical characteristics of surface plasmon resonance-based optical sensor for the detection of hydrogen peroxide

https://doi.org/10.1515/gps-2023-0070
received April 19, 2023; accepted July 24, 2023

Abstract: Silver nanoparticles (AgNPs) have been efficaciously synthesized from $AgNO_3$ *via* an easy and green method, also called green synthesis, using Mon Thong durian (*Durio zibethinus* L.) rind extract. The inner shell of durian rind extract was used as an intermediary for the synthesis of AgNPs because the absorption spectra of the AgNP colloid extracted from the inner shell had a higher absorption than that of the outer shell. Additionally, we have found more fructose and glucose – which act as a reducing agent – and protein and carbohydrates – which act as the stabilizer – in a higher amount in the inner shell than the extract from the outer shell. The synthesized AgNPs were mainly spherical in shape and exhibited a relatively narrow size distribution with an average particle diameter of 10.2 ± 0.2 nm. In the reduction of hydrogen peroxide (H_2O_2), these nanoparticles demonstrate catalytic activity. The degradation of AgNPs, including the catalytic decomposition of H_2O_2, causes a considerable change in the absorbance strength of the surface plasmon resonance band depending on the H_2O_2 concentration. Over a broad concentration range of 10^{-1}–10^{-6} mol·L^{-1} H_2O_2, a good sensitivity and a linear response are achieved. This sensor's quantification limit is found to be 0.9 μmol·L^{-1} H_2O_2. Therefore, this optical sensor for the detection of H_2O_2 can be potentially applied in the determination of color indicators in medical or clinical diagnosis, biochemical analysis, and environmental applications.

Keywords: durian rind extract, green synthesis, hydrogen peroxide sensor, silver nanoparticles, surface plasmon resonance

1 Introduction

Considering that hydrogen peroxide (H_2O_2) is a byproduct of processes mediated by several oxidase enzymes, determining H_2O_2 in trace amounts is a crucial and essential task. It is crucial in a variety of industries, including those related to food, medicine, clinical laboratories, and environmental analysis [1,2]. The majority of the techniques for measuring H_2O_2 that have been developed until now are based on enzymes and include spectrofluorometry [3–5], spectrophotometry [6–8], and electrochemistry [9–11]. Although enzyme sensitivity and selectivity are exceptional, immobilizing and stabilizing enzymes are challenging operations. It was found that sensors had poor repeatability and instability when exposed to enzymatic H_2O_2.

The construction of innovative devices and applications, including chemical sensors and biosensors, is made possible by the distinctive optical, magnetic, catalytic, and mechanical capabilities of nanoscale materials [12–15]. According to recent publications [16–19], several attempts have been made to monitor the concentration of H_2O_2 electrochemically by applying nanomaterials (using no enzymes). Due to their advantages such as high surface response activity, high catalytic efficiency, high surface-to-volume ratio, strong adsorption ability, stability, and ease of electron transfer, nanomaterial-altered electrodes are an excellent option for detecting H_2O_2. The sensors made of nanomaterials have quicker reaction times and lower detection thresholds [20]. Platinum [21,22], silver [23–26], gold [27], copper oxide [28], MnOOH [29], or silver nanoparticles (AgNPs) encapsulated in SBA-15 mesoporous silica [30] and electrodeposited on a ZnO film [31] are only a few examples of the

* **Corresponding author: Kheamrutai Thamaphat**, Green Synthesis and Application Laboratory, Applied Science and Engineering for Social Solution Research Unit, Department of Physics, Faculty of Science, King Mongkut's University of Technology Thonburi, Bangkok 10140, Thailand, e-mail: kheamrutai.tha@kmutt.ac.th
Fueangfakan Chutrakulwong: Division of Physics, Faculty of Science and Technology, Rajamangala University of Technology Krungthep, Bangkok 10120, Thailand

metal or metal oxide nanoparticle-based electrodes that have been chemically changed. H_2O_2 can be detected using electro-analytical techniques.

The optical sensors and biosensors based on the localized surface plasmon resonance (LSPR), which may be emitted by nanostructured noble metals like gold and silver, are an excellent, quick, and low-cost substitute for amperometric nanostructured sensors [32]. Briefly, the passage of electrons through the interior metal framework gets constrained when the size of a metal form shrinks from the bulk scale to the nanoscale. As a result, when incident light enters resonance with the conduction band electrons on the surfaces of metallic nanoparticles, distinct absorption bands of their UV-visible (UV-Vis) spectrum are shown. It merely referred to these oscillations in charge density as LSPR [33]. According to Endo and colleagues [34–38], gold nanoparticles are specifically employed for LSPR excitation and the development of corresponding optical biosensors in medical and food applications. AgNPs have a catalytic activity for the breakdown of H_2O_2, according to a number of recent research studies [23,39]. Endo et al. [40] and Alzahrani [41] synthesized polyvinylpyrrolidone-coated AgNPs based on an LSPR-based fully optical detection method for the quantitative determination of reactive oxygen species, particularly H_2O_2. AgNPs with poly(vinyl alcohol) (PVA) caps as a renewable LSPR-based sensor for H_2O_2 detection and measurement have been suggested by Filippo and colleagues [42].

To obtain silver colloids with nanostructures, wet chemical synthesis was frequently used [43]. Numerous nanomaterial preparations entail hazardous chemicals, poor material conversion, high energy demands, and time-consuming, inefficient purifications. Here, we instead synthesize AgNPs using a green method. There has already been some advancement in the creation of green chemistry that is safe, non-toxic, and acceptable to the environment for the production of noble metal (gold and silver) nanoparticles. For the synthesis of Au and Ag nanoparticles, green reducing agents such as citrate [44–46], glucose [47–51], ascorbic acid [52], and hydrogen peroxide [53–55] have been investigated. AgNPs can be made using water-soluble polymers, such as gum Arabic, gelatin, PVA, and methyl hydroxyethyl cellulose [46,56–59]. Starch has recently been used as a green capping agent [48–50]. Mehata [60] and Ghaseminezhad et al. [61] have published many studies on green synthesis, while Mouzaki and colleagues have provided an overview of the synthesis of AgNPs [62].

We used Mon Thong durian (*Durio zibethinus* L.) rind extract [63] as a reducing agent and stabilizer to reduce Ag^+ dissolved in $AgNO_3$ solution to AgNPs with a narrow size distribution and demonstrated their applicability as an LSPR-based optical sensor due to the current development on green synthesis techniques for preparing metallic nanoparticles as well as on LSPR based on detection techniques and sensing devices. We make use of the fact that the analyte, H_2O_2, can be used as an active oxidant for AgNPs and demonstrate that, under suitable experimental conditions, the change in the LSPR absorbance strength caused by the degradation of the as-prepared AgNPs correlates well with the concentration of H_2O_2. These nanoparticles serve as an unconventional LSPR-based optical sensor that we employ to measure H_2O_2.

2 Materials and methods

2.1 Preparation of durian rind extract

The Mon Thong durian rinds were used throughout this work. The fresh durian rinds collected during the durian season from the fruit market were cleaned, dried, and the outer layer from the inner layer was separated. Then, it was ground to powder, stored in a vacuum box, and placed at −20°C until it was used to prepare durian rind extract.

About 50 g of the durian outer layer powder was used to prepare the durian rind extract. The powder was boiled in 500 mL of deionized (DI) water for 30 min. The resulting extract was filtered through Whatman filter paper No. 1 with a pore size of 11 μm. The preparation of the inner layer of durian rind extract was the same as that of the outer layer. We stored this extract at 4°C for further experiments.

2.2 Solutions used in the experiment

$AgNO_3$ was used as a substrate for the synthesis of AgNPs using the reduction method. NaOH and HCl solutions were used for adjusting the pH change. $AgNO_3$ was purchased from Poch. When $AgNO_3$ was dissolved in DI water, it caused the dissociation of Ag^+, which acts as an electron acceptor (oxidizer) in the reduction process.

2.3 Synthesis of AgNP colloid using durian rind extract as a reducing agent and stabilizer

In this experiment, durian rind was used to synthesize environmentally friendly AgNPs using the Mon Thong durian extract as both a reducing agent and stabilizer. The durian extract will act as the electron distributor to the dissociated Ag^+ in $AgNO_3$ solution under light conditions as a catalyst. The process is shown as represented by Eqs. 1 and 2:

$$AgNO_3(s) \xrightarrow{H_2O} Ag^+(aq) + NO_3^-(aq) \tag{1}$$

$$Ag^+(aq) + e^- \xrightarrow{light} Ag\ (s) \tag{2}$$

First, 30 mL of the durian outer shell extract was mixed with 30 mL of 1 mM $AgNO_3$ solution (1:1 ratio), and the pH of the solution was adjusted to 8.5. The solution was stirred with a magnetic stirrer (Stuart, CB 162) for 3 h at a light intensity of 13,430 lux and a temperature of 25 ± 1°C. The absorbance of the solution was measured in the wavelength range of 300–800 nm with a UV-Vis spectrophotometer (Avantes, AvaSpec-2048). The light source used was a tungsten–deuterium lamp, which generated light in the wavelength range of 177–1,100 nm. The absorbance of the solution was measured by adjusting the absorbance measurement mode (A). The extracted water from durian rind was used as a blank. The same process was repeated but the durian inner shell extract was used instead of the durian outer shell extract.

2.4 Characterization of AgNPs synthesized with the durian rind extract

The AgNPs synthesized with durian rind extract were tested for their qualitative and quantitative characteristics as follows:

- UV-Vis spectrophotometer was employed to examine the absorbance of AgNPs synthesized with the extract obtained from the inner and outer shells of durian rind.
- TEM (JEOL, JEM-2100) was used to examine the dispersion and shape of the AgNPs.
- XRD (Bruker, D8 Advance) was used to analyze the crystalline structure of the elements.
- SEM-EDX (JEOL, JSM-6610LV) was used to determine the elemental composition of AgNPs.

2.5 Optical characteristics of the surface plasmon resonance (SPR)-based optical sensor for the detection of H_2O_2 of AgNP

To evaluate the optical characteristics of AgNP solution as SPR-based H_2O_2 sensor, 3% of different concentrations of

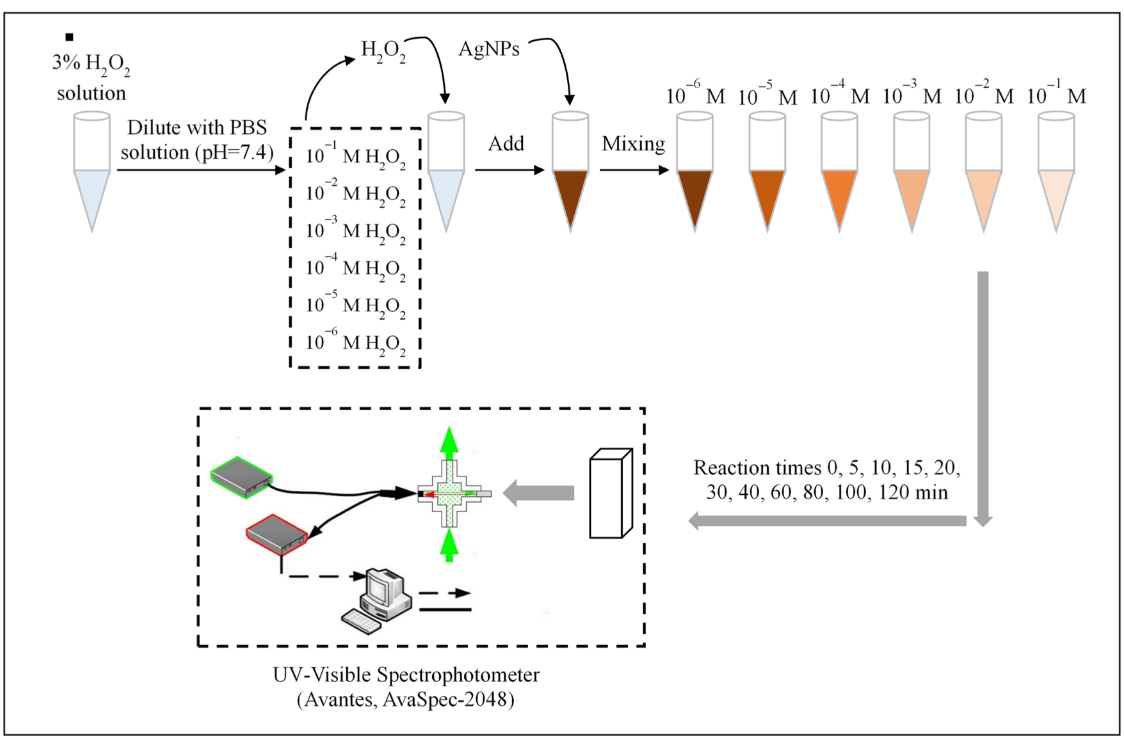

Figure 1: Experimental procedure for SPR optical characterization of colloid AgNPs synthesized from the durian rind extract.

H_2O_2 solutions diluted with phosphate buffer (pH 7.4) were introduced into the AgNP solution in the quartz cuvette at a ratio of 1:1.5. The change in its optical characteristics with time (0, 5, 10, 15, 20, 30, 40, 60, 80, 100, and 120 min) in the visible range (350–850 nm) was monitored by a UV-Vis spectrophotometer (Avantes, AvaSpec-2048), as shown in Figure 1.

3 Results and discussion

3.1 Durian rind extract and the conditions used in the AgNP synthesis

Before synthesizing AgNPs, the absorbance of durian rind extracted from outer and inner shells was measured. The results showed that the durian extract from the outer shell of durian rind had the highest absorbance at 320.896 nm. In contrast, the extract from the inner shell had the highest absorption at a wavelength of 323.689 nm, which was higher than that from the outer shell. Therefore, the inner shell extract was used to synthesize AgNPs.

In this experiment, the inner shell of the durian rind extract was used as an intermediary for the synthesis of AgNPs because the AgNP colloid extracted from the inner shell had a higher absorption than that of the outer shell. Moreover, the durian inner shell yielded more AgNPs than the outer shell (as presented in Figure 2). Additionally, we have found more fructose and glucose – which act as a reducing agent – and protein and carbohydrates – which act as the stabilizer – in a higher amount than the extract from the outer shell (as shown in Table 1).

Table 1: Nutrient contents in durian rind

Substance	Substance content in the outer shell	Substance content in the inner shell
Fructose	0.93 g·100 g^{-1}	8.01 g·100 g^{-1}
Glucose	1.01 g·100 g^{-1}	2.17 g·100 g^{-1}
Protein	0.09 g·100 mL^{-1}	0.03 g·100 mL^{-1}
Carbohydrate	0.43 g·100 mL^{-1}	1.13 g·100 mL^{-1}

Therefore, at this stage, the extract from the inner shell of durian rind was recommended as a reducing agent and a stabilizer in the synthesis of AgNPs.

3.2 Effect of reaction times on the absorbance of colloid AgNPs

AgNPs were synthesized using the inner durian rind extract at a light intensity of 13,430 lux with the pH of the solution adjusted to 8.5. Then, the absorbance of the solutions was measured at reaction times of 5, 10, 30 min, 1, 2, 3, 6, 9, and 12 h with a UV-Vis spectrophotometer. With the formation of AgNPs, the color of the solution changed from light yellow (source extract) to yellowish-brown because of the reduction of Ag^+ ions in AgNPs as the reaction time was increased gradually up to 12 h, as shown in Figure 3.

As observed in Figure 3, the color of AgNPs synthesized using the inner durian rind extract at a light intensity of 13,430 lux and pH 8.5 had a yellowish-brown color at all reaction times. This result implies that the higher the absorbance, the higher the quantity of AgNPs. Therefore,

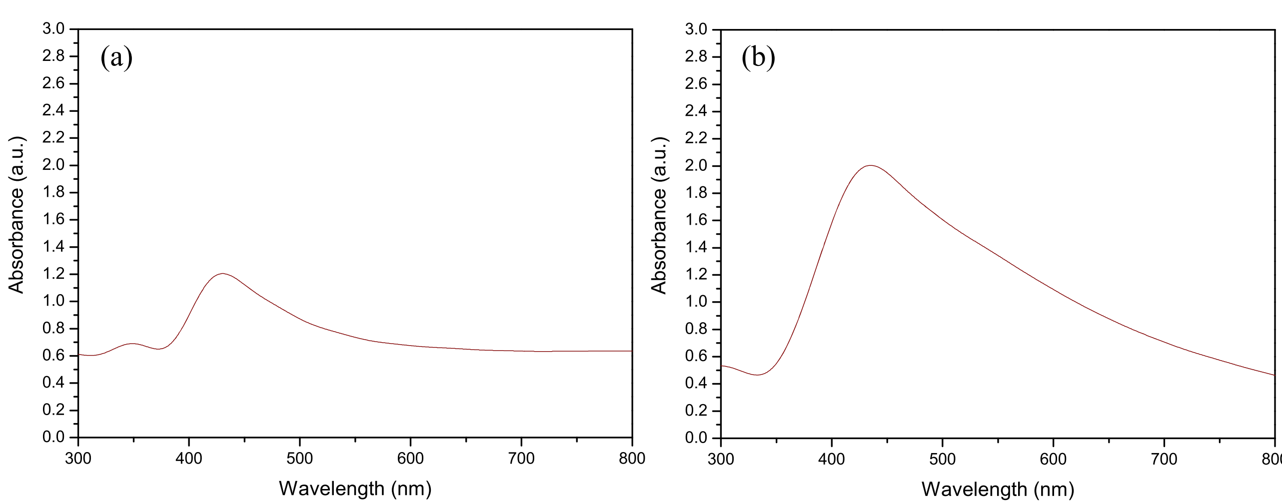

Figure 2: Colloid absorbance of AgNPs synthesized using the durian rind extract: (a) outer shell of durian rind and (b) inner shell of durian rind (pH = 8.5; reaction time, 3 h) at a light intensity of 13,430 lux.

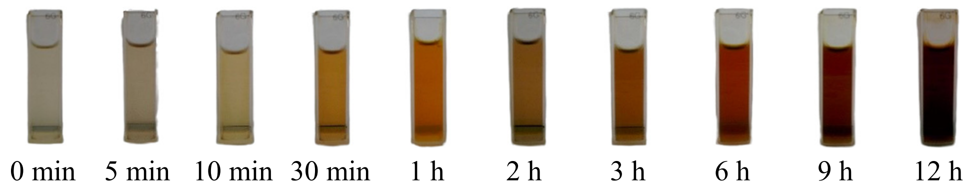

Figure 3: Colors of colloids of AgNPs synthesized using an extract from the inner durian rind at a light intensity of 13,430 lux, pH of 8.5, and reaction times of 0 min to 12 h.

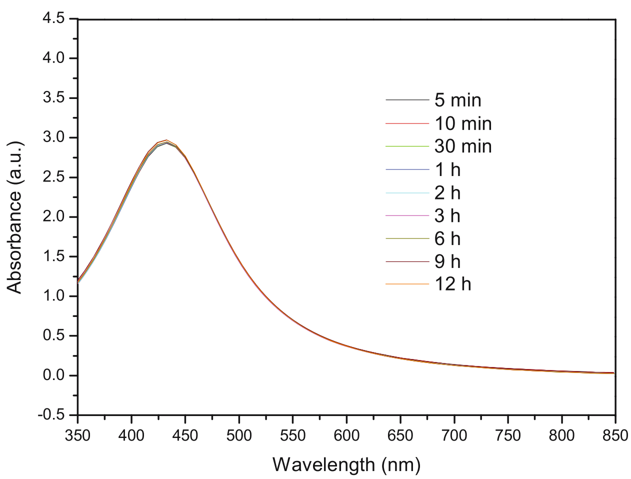

Figure 4: Colloidal absorbance of AgNPs synthesized using an extract from the inner durian rind at a light intensity of 13,430 lux, pH of 8.5, and reaction times of 5 min to 12 h.

adjusting the pH of the solution to 8.5 is recommended for synthesizing AgNPs as it generates a higher quantity.

As observed in Figure 4, at a pH of 8.5, the absorbance of the synthesized AgNPs had the highest at 416 nm, which implied the small size of AgNPs. Therefore, adjusting the pH of the solution to 8.5 was recommended in synthesizing AgNPs using an extract from the inner shell of durian rind.

Figure 4 shows the UV-Vis spectrum recorded from the formation of AgNPs in solution. The appearance of a strong and sharp plasmon band at a wavelength of maximum absorbance (λ_{max}) of 416 nm shows the formation of AgNP colloids. The reaction was completed within 3 h, which can be ascertained by no change in the absorbance. This value of λ_{max} was blue-shifted toward a shorter wavelength of approximately 416 nm at a pH value of 8.5 and the full-width at half-maximum (FWHM) of the absorbance band was 122 nm.

3.3 Dispersion, shape, and size of AgNPs

TEM (JEOL, JEM-2100) was employed to investigate the formation of dispersion and shape of AgNPs synthesized using an extract from the inner durian rind at a light intensity of 13,430 lux and a reaction time of 12 h at a pH of 8.5. The smallest size of AgNPs is shown in Figure 5. Therefore, it

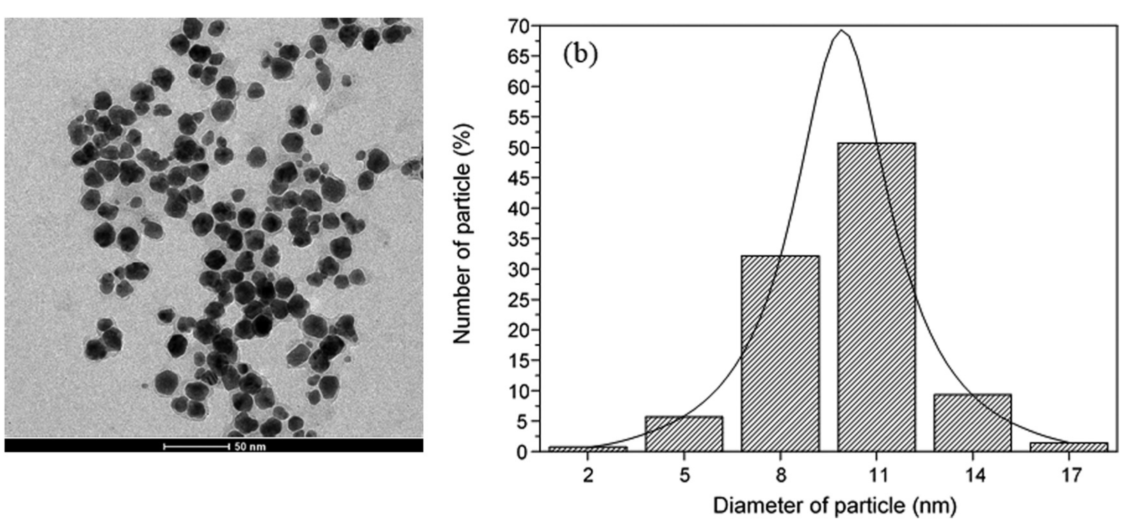

Figure 5: TEM analysis results: (a) TEM image of AgNPs synthesized from 1 mM $AgNO_3$ solution and durian rind extract at ambient conditions (solution pH = 8.5) and (b) corresponding particle size distribution histogram of AgNPs.

can be concluded that the pH of the solution used in the AgNP synthesis (the inner shell of durian rind extract and $AgNO_3$) should be adjusted to 8.5 to get the smallest size of AgNPs.

The TEM results are shown in Figure 5a, which displays that AgNPs are formed in spherical shapes. Figure 5b shows a relatively narrow size distribution with an average diameter of 10.2 ± 0.2 nm, which corresponds to the XRD pattern, as illustrated in Figure 6. Figure 6 shows the XRD patterns of AgNPs synthesized using the durian rind extract. The XRD pattern shows the sharp peaks of the face-centered cubic (fcc) crystal structure (JCPDS file no.04-0783) with diffraction peaks at 37°, 44°, 64°, and 77° in the 2θ range of 20–80°, which correspond to the (111), (200), (220), and (311) facets of silver, respectively. Therefore, the UV-Vis spectra, TEM images, and XRD patterns are strong evidence to confirm that the method described here is an effective approach for the synthesis of AgNPs. Additionally, EDX analysis was used to estimate the elemental composition of AgNPs. Figure 7 shows that the energy of the elemental silver peak is 3 keV.

3.4 Optical characteristics of the SPR-based optical sensor for the detection of H_2O_2 of AgNPs

3.4.1 Effect of reaction times on the wavelength and absorbance spectra of dilute H_2O_2 solution

Dilute H_2O_2 (10^{-2} M) was used to determine the effect of reaction times on the wavelength and absorbance of dilute H_2O_2 solution. The results are shown in Figure 8.

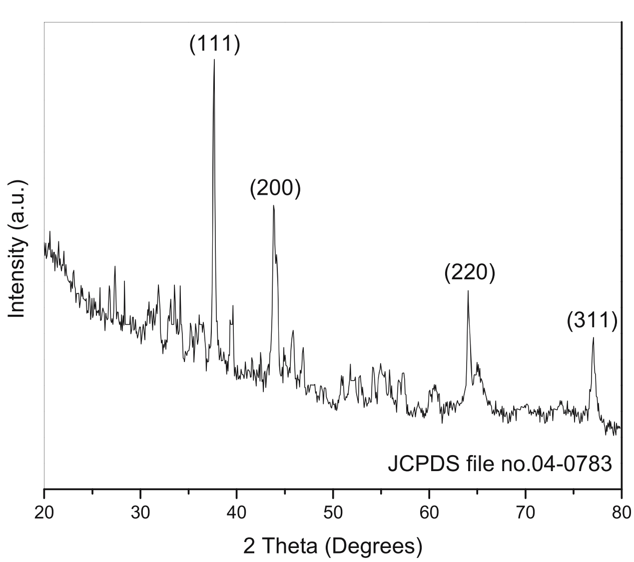

Figure 6: X-ray diffraction patterns of the synthesized AgNPs.

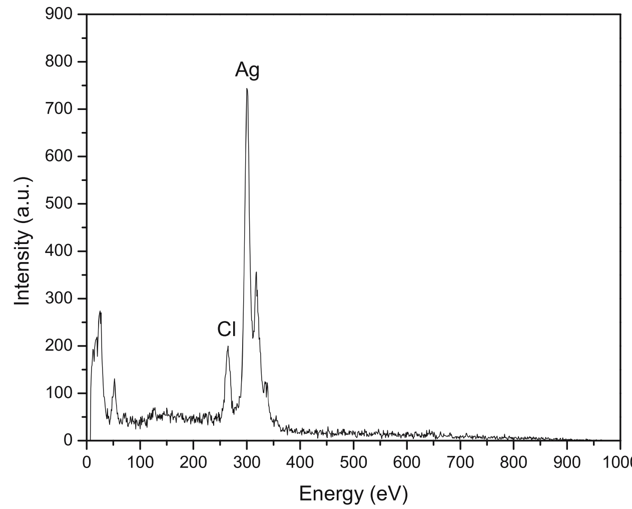

Figure 7: SEM-EDX spectrum of the synthesized AgNPs confirming the presence of silver.

From Figure 8, the maximum absorbance of 10^{-2} M H_2O_2 is at 416 nm, which implies that the lesser the reaction time, the higher the absorbance of dilute H_2O_2.

In order to determine the effect of dilution on the SPR absorbance strength, we introduced phosphate buffer into the AgNP colloid at a ratio of 1:1.5. The change in the absorbance strength at λ_{max} is because of its dependence on the AgNP concentration. In this experiment, the dilution with buffer solution affects the AgNP concentration. As a result, a volume ratio of H_2O_2/colloid AgNPs is chosen as 1:1.5 to evaluate the characteristics of the SPR-based sensor.

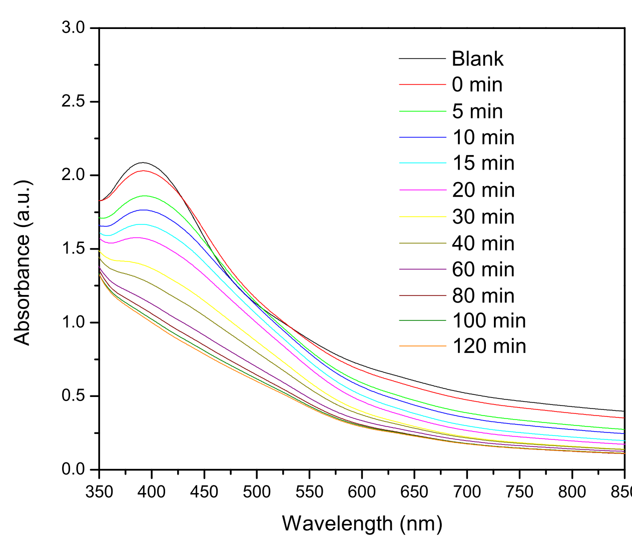

Figure 8: Changes in the SPR absorbance strength with time and the addition of 10^{-2} M H_2O_2 solution in the as-synthesized AgNPs solution at a volume ratio of 1:1.5.

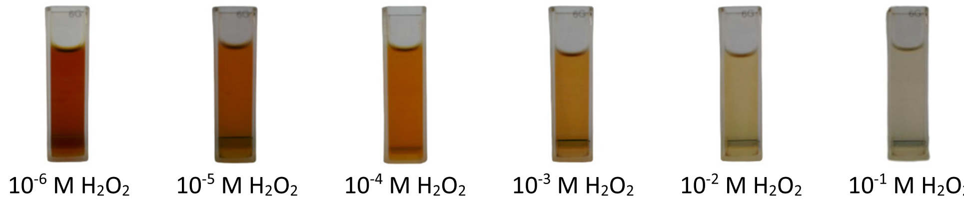

Figure 9: Colors of H_2O_2 and AgNP solution at different H_2O_2 concentrations.

3.4.2 Concentration of H_2O_2 and absorbance of the solution

UV-Vis spectrophotometry was employed to determine the absorbance of H_2O_2 and AgNP solution at different H_2O_2 concentration levels and a reaction time of 15 min (as shown in Figure 9).

As shown in Figure 9, the color of H_2O_2 and AgNP solution faded as the concentration of H_2O_2 increased. This finding implies that the higher the concentration of H_2O_2 in the solution, the fadedness of the color of the solution increased.

The spectroscopy measurements showed the formation of AgNPs. The AgNP synthesis was verified by UV-Vis spectroscopy by determining the maximum absorbance at approximately 416 nm because of the SPR. Figure 10 represents the SPR peak at 416 nm of AgNPs, showing a sufficient dispersion, narrow size distribution, and the spherical shape of AgNPs. The addition of 1 mL of 3% H_2O_2 solution with different volumes of AgNPs leads to a decrease in the SPR absorbance of the AgNPs, leading to the bleaching of the brownish color to a clear solution of AgNPs.

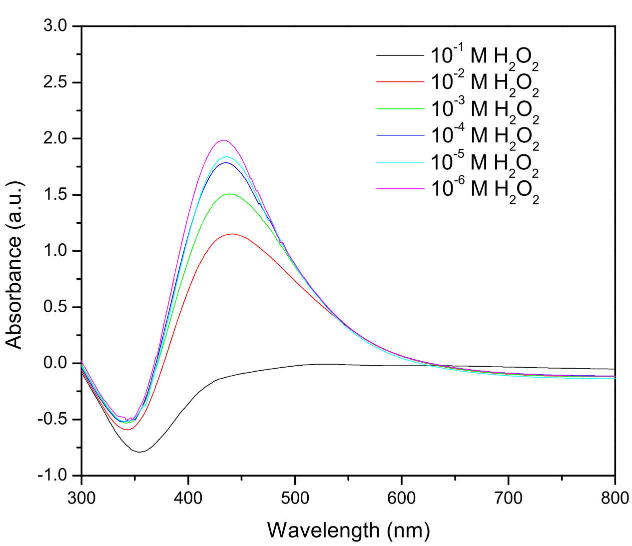

Figure 10: UV-Vis absorption spectra recorded for 15 min after the addition of different concentrations of H_2O_2 solution to the solution of AgNPs at a volume ratio of 1:1.5.

3.4.3 Effect of time on changes in the reaction of AgNPs and H_2O_2 solution at different concentrations

UV-Vis spectrophotometry was employed to analyze the effect of reaction time on changes in the reaction of AgNPs and H_2O_2 solution at different concentrations, and the results are shown in Figure 11.

As observed in Figure 11, absorption shows relatively significant changes in the reactions between different concentrations of AgNPs and dilute H_2O_2 solutions between 0 and 15 min. However, it was found that the reactions became static after 15 min. This reaction pattern represents the reactions of different concentrations of AgNPs and dilute H_2O_2 solution, as observed in Figure 11. Therefore, 15 min of reaction time was recommended to apply for AgNPs (extracted from the inner layer of durian rind) to an SPR-based optical sensor for the detection of H_2O_2. The $(A_0 - A_t)/A_0$ values calculated at a reaction time of 15 min and the concentration of H_2O_2 are presented in Figure 12. As seen, the absorbance change at a reaction time decreases proportionally to the H_2O_2 concentration. It can be concluded that the optical sensor studied using the durian rind extract in synthesizing AgNPs ensures a linear response

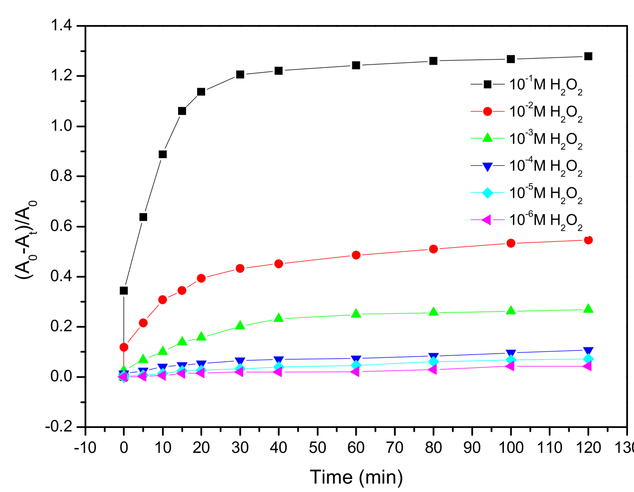

Figure 11: The relative changes in the reaction of AgNPs and H_2O_2 solution at a 15 min reaction time at different concentrations of H_2O_2 solution.

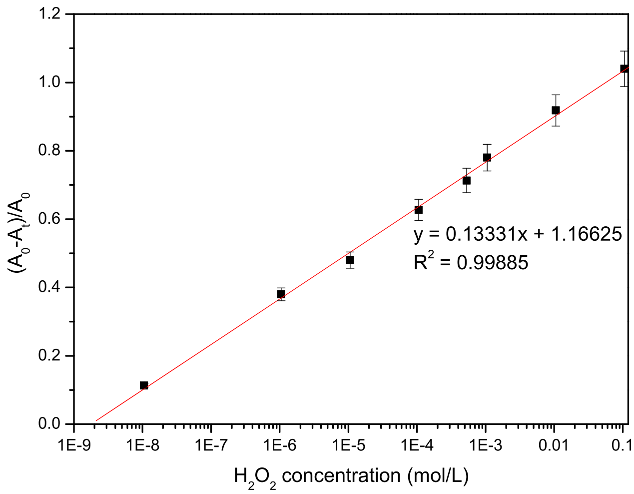

Figure 12: Relative change in the absorbance strength of the AgNP solution 15 min after the addition of H_2O_2 solution as a function of H_2O_2 concentration.

over the wide concentration range of 10^{-1}–10^{-6} mol·L^{-1} H_2O_2 and might be successfully applied in analytical procedures for the determination of H_2O_2 in various samples such as vegetables and food. The quantification limit, calculated based on the criteria, is 0.9 µmol·L^{-1}.

Comparing the H_2O_2 detection performance of AgNPs extracted from durian rind with previous studies, we found that AgNPs obtained from the durian extract in our study had the lowest detection limit compared to other methods (Table 2) [24].

3.4.4 Mechanism of H_2O_2 detection

From Eqs. 1 and 2, the durian rind extract can be reduced to Ag^+ to Ag^0 because it is composed of water-soluble polysaccharides that comprise a linear chain of several hundred to over ten thousand β (1 → 4) linked D-glucose units and low protein content [67]. Glucose generally acts as a reducing agent in the preparation process of AgNPs. After these simple steps, the optical sensor is ready for use.

With the addition of another strong oxidizing agent as H_2O_2, the reverse process occurs, in which AgNPs are oxidized with the consequent formation of silver oxide, and peroxide is decomposed into water and oxygen [68]. The oxi-reduction occurs as described by the following chemical equations (Eqs. 3 and 4):

$$2Ag(s) + H_2O_2(ag) \rightarrow 2Ag^+(aq) + 2OH^-(aq) \quad (3)$$

$$2Ag^+(aq) + 2OH^-(aq) \rightarrow Ag_2O\,(s) + H_2O\,(l) \quad (4)$$

We observed that the intensity of the yellowish-brown color decreases with increasing H_2O_2 concentration (Figure 9), which is attributed to the oxidation of Ag^0.

4 Conclusions and future directions

In this work, we have demonstrated a challenging alternative for the synthesis of AgNPs using the bio-waste durian rind as a low-cost biological reducing agent. By using this strategy, agricultural wastes may be used more effectively and the garbage that could have an adverse effect on the environment can be disposed of. The effective utilization of the hydroxyl groups of glucose as a reducing agent and starch or protein as a stabilizer may contribute to the green production of AgNPs from durian rind. Only spherical particles were formed, with an average diameter of 10.2 ± 0.2 nm.

Our synthesis produced AgNPs with an SPR band at 416 nm, good colloidal AgNP stability, and intermediate catalytic activity for the oxidation of H_2O_2. The SPR band's absorbance intensity significantly varies depending on the H_2O_2 concentration due to the degradation of AgNPs due to the catalytic breakdown of H_2O_2. An SPR-based sensor for the detection of H_2O_2 is suggested based on this technique. This sensor responds linearly and with exceptional sensitivity throughout a wide range of 10^{-1}–10^{-6} mol·L^{-1} H_2O_2. The quantitative limit of detection, according to our findings, is 0.9 µmol·L^{-1} H_2O_2. The application of an SPR-based optical sensor for H_2O_2 detection and for the detection of other reactive oxygen species is possible.

Table 2: Comparison of analytical performances of the methods for the determination of H_2O_2

Method	Detection limit (µM)	Linear range	References
Decomposition of particles	10	N/A	[64]
Decomposition of particles	1.60	10–80 µM	[65]
Decomposition of particles	5	10–40 µM	[66]
Decomposition of particles	112	60–600 µM	[24]
Decomposition of particles	0.9	1 µM to 0.1 M	This work

H_2O_2 is a crucial chemical used in many industrial processes including textile, pharmaceutical, culinary, cleaning, and disinfection. As mentioned above, H_2O_2 detection is effective over a wide range of concentrations. For these sensors to be extensively used in the aforementioned industrial applications, we still need to improve in terms of sensitivity and selectivity for H_2O_2 in varied samples. AgNPs are a type of nanomaterial that is used to enhance the performance of sensors in various environmental conditions. To allow continuous monitoring necessary for industrial applications, further efforts will need to be made to address the sensor contamination concerns in various sample types. In conclusion, the flexible detection range, straightforward construction technique, and affordable price of optical sensors make them suitable for a variety of applications.

Acknowledgements: The authors would like to thank the Division of Physics, Faculty of Science and Technology, Rajamangala University of Technology Krungthep and Green Synthesis and Application Laboratory, Applied Science and Engineering for Social Solution Research Unit, Department of Physics, Faculty of Science, King Mongkut's University of Technology Thonburi for providing measuring equipment. The authors are grateful to the Department of Chemistry, Faculty of Science, Mahidol University, for providing XRD measurement.

Funding information: The authors state no funding was involved.

Author contributions: Fueangfakan Chutrakulwong: conceptualization, data curation, formal analysis, resources, validation, writing – original draft, and writing – review and editing; Kheamrutai Thamaphat: conceptualization, methodology, resources, supervision, validation, and writing – review and editing.

Conflict of interest: The authors state no conflict of interest.

Data availability statement: The datasets generated and analysed during the current study are available from the corresponding author on reasonable request.

References

[1] Perry SC, Pangotra D, Vieira L, Csepei LI, Sieber V, Wang L, et al. Electrochemical synthesis of hydrogen peroxide from water and oxygen. Nat Rev Chem. 2019;3(1):442–58. doi: 10.1038/s41570-019-0110-6.

[2] Wang J, Lin Y, Chen L. Organic-phase biosensors for monitoring phenol and hydrogen peroxide in pharmaceutical antibacterial products. Analyst. 1993;118(3):277–80. doi: 10.1039/an9931800277.

[3] Manzoori J, Amjadi M, Orooji M. Application of crude extract of kohlrabi (Brassica oleracea gongylodes) as a rich source of peroxidase in the spectrofluorometric determination of hydrogen peroxide in honey samples. Anal Sci. 2006;22(9):1201–6. doi: 10.2116/analsci.22.1201.

[4] Tang B, Zhang L, Xu K. FIA-near-infrared spectrofluorimetric trace determination of hydrogen peroxide using tricarchlorobocyanine dye (Cy.7.Cl) and horseradish peroxidase (HRP). Talanta. 2006;68(3):876–82. doi: 10.1016/j.talanta.2005.06.053.

[5] Hitomi Y, Takeyasu T, Funabiki T, Kodera M. Detection of enzymatically generated hydrogen peroxide by metal-based fluorescent probe. Anal Chem. 2011;83(24):9213–6. doi: 10.1021/ac202534g.

[6] Wei H, Wang E. Fe_3O_4 magnetic nanoparticles as peroxidase mimetics and their applications in H_2O_2 and glucose detection. Anal Chem. 2008;80(6):2250–4. doi: 10.1021/ac702203f.

[7] Chang Q, Deng K, Zhu L, Jiang G, Yu C, Tang H. Determination of hydrogen peroxide with the aid of peroxidase-like Fe_3O_4 magnetic nanoparticles as the catalyst. Microchim Acta. 2009;165(3):299–305. doi: 10.1007/s00604-008-0133-z.

[8] Hsu CC, Lo YR, Lin YC, Shi YC, Li PL. A spectrometric method for hydrogen peroxide concentration measurement with a reusable and cost-efficient sensor. Sensors. 2015;15(10):25716–29. doi: 10.3390/s151025716.

[9] Jin GH, Ko E, Kim MK, Tran VK, Son SE, Geng Y, et al. Graphene oxide-gold nanozyme for highly sensitive electrochemical detection of hydrogen peroxide. Sensor Actuat B Chem. 2018;274(1):201–9. doi: 10.1016/j.snb.2018.07.160.

[10] Chen S, Yuan R, Chai Y, Hu F. Electrochemical sensing of hydrogen peroxide using metal nanoparticles: A review. Microchim Acta. 2013;180(1-2):15–32. doi: 10.1007/s00604-012-0904-4.

[11] Zhang R, Chen W. Recent advances in graphene-based nanomaterials for fabricating electrochemical hydrogen peroxide sensors. Biosens Bioelectron. 2017;89(Pt 1):249–68. doi: 10.1016/j.bios.2016.01.080.

[12] Beck F, Loessl M, Baeumner AJ. Signaling strategies of silver nanoparticles in optical and electrochemical biosensors: considering their potential for the point-of-care. Microchim Acta. 2023;190(3):1–19. doi: 10.1007/s00604-023-05666-6.

[13] Imran M, Ehrhardt CJ, Bertino MF, Shah MR, Yadavalli VK. Chitosan stabilized silver nanoparticles for the electrochemical detection of lipopolysaccharide: A facile biosensing approach for Gram-negative bacteria. Micromachines. 2020;11(4):1–12. doi: 10.3390/mi11040413.

[14] Santos VM, Ribeiro RSA, Bosco AJT, Alhadeff EM, Bojorge NI. Characterization and evaluation of silver-nanoparticle-incorporated in composite graphite aiming at their application in biosensors. Braz J Chem Eng. 2017;34(3):647–57. doi: 10.1590/0104-6632.20170343s20150649.

[15] Xing Y, Feng XZ, Zhang L, Hou J, Han GC, Chen Z. A sensitive and selective electrochemical biosensor for the determination of beta-amyloid oligomer by inhibiting the peptide-triggered in situ assembly of silver nanoparticles. Int J Nanomed. 2017;12:3171–9. doi: 10.2147/IJN.S132776.

[16] Li X, Liu Y, Zheng L, Dong M, Xue Z, Lu X, et al. A novel nonenzymatic hydrogen peroxide sensor based on silver nanoparticles and ionic liquid functionalized multiwalled carbon nanotube composite

modified electrode. Electrochim Acta. 2013;113:170–5. doi: 10.1016/j.electacta.2013.09.049.
[17] Yang YQ, Xie HL, Tang J, Tang S, Yi J, Zhang HL. Design and preparation of non-enzymatic hydrogen peroxide sensor based on a novel rigid chain liquid crystalline polymer/reduced graphene oxide composite. RSC Adv. 2015;5(78):63662–8. doi: 10.1039/C5RA10540D.
[18] Thanh TD, Balamurugan J, Lee SH, Kim NH, Lee JH. Novel porous gold-palladium nanoalloy network-supported graphene as an advanced catalyst for non-enzymatic hydrogen peroxide sensing. Biosens Bioelectron. 2016;85(3):669–78. doi: 10.1016/j.bios.2016.05.075.
[19] Yang K, Yan Z, Ma L, Du Y, Peng B, Feng J. A facile one-step synthesis of cuprous oxide/silver nanocomposites as efficient electrode-modifying materials for nonenzyme hydrogen peroxide sensor. Nanomaterials. 2019;9(4):1–14. doi: 10.3390/nano9040523.
[20] Hahn JI, Lieber CM. Direct ultrasensitive electrical detection of DNA and DNA sequence variations using nanowire nanosensors. Nano Lett. 2004;4(1):51–4. doi: 10.1021/nl034853b.
[21] You T, Niwa O, Tomita M, Hirono S. Characterization of platinum nanoparticle-embedded carbon film electrode and its detection of hydrogen peroxide. Anal Chem. 2003;75(9):2080–5. doi: 10.1021/ac026337w.
[22] Han JH, Boo H, Park S, Chung TD. Electrochemical oxidation of hydrogen peroxide at nanoporous platinum electrodes and the application to glutamate microsensor. Electrochim Acta. 2006;52(4):1788–91. doi: 10.1016/j.electacta.2005.12.060.
[23] Raoof JB, Ojani R, Hasheminejad E, Rashid-Nadimi S. Electrochemical synthesis of Ag nanoparticles supported on glassy carbon electrode by means of p-isopropyl calix[6]arene matrix and its application for electrocatalytic reduction of H_2O_2. Appl Surf Sci. 2012;258(7):2788–95. doi: 10.1016/j.apsusc.2011.10.133.
[24] Teodoro KBR, Migliorini FL, Christinelli WA, Correa DS. Detection of hydrogen peroxide (H_2O_2) using a colorimetric sensor based on cellulose nanowhiskers and silver nanoparticles. Carbohyd Polym. 2019;212(3):235–41. doi: 10.1016/j.carbpol.2019.02.053.
[25] Reyes DF. Green-synthesized silver nanoparticles as sensor probes for the naked-eye detection of hydrogen peroxide. Orient J Chem. 2020;36(4):640–4. doi: 10.13005/ojc/360407.
[26] Elgamouz A, Idriss H, Nassab C, Bihi A, Bajou K, Hasan K, et al. Green synthesis, characterization, antimicrobial, anti-cancer, and optimization of colorimetric sensing of hydrogen peroxide of algae extract capped silver nanoparticles. Nanomaterials. 2020;10(9):1–19. doi: 10.3390/nano10091861.
[27] Cui H, Wang W, Duan CF, Dong YP, Guo JZ. Synthesis, characterization, and electrochemiluminescence of luminol-reduced gold nanoparticles and their application in a hydrogen peroxide sensor. Chem Eur J. 2007;13(24):6975–84. doi: 10.1002/chem.200700011.
[28] Yang G, Chen F, Yang Z. Electrocatalytic oxidation of hydrogen peroxide based on the shuttlelike nano-CuO-modified electrode. Int J Electrochem. 2012;2012:1–6. doi: 10.1155/2012/194183.
[29] Xu W, Liu J, Wang M, Chen L, Wang X, Hu C. Direct growth of MnOOH nanorod arrays on a carbon cloth for high-performance non-enzymatic hydrogen peroxide sensing. Anal Chim Acta. 2016;913:128–36. doi: 10.1016/j.aca.2016.01.055.
[30] Lin DH, Jiang YX, Wang Y, Sun SG. Silver nanoparticles confined in SBA-15 mesoporous silica and the application as a sensor for detecting hydrogen peroxide. J Nanomater. 2008;2008(1):1–10. doi: 10.1155/2008/473791.
[31] Wang Q, Zheng J. Electrodeposition of silver nanoparticles on a zinc oxide film: improvement of amperometric sensing sensitivity and stability for hydrogen peroxide determination. Microchim Acta. 2010;169(3–4):361–5. doi: 10.1007/s00604-010-0356-7.
[32] Kim DM, Park JS, Jung SW, Yeom J, Yoo SM. Biosensing applications using nanostructure-based localized surface plasmon resonance sensors. Sensors. 2021;21(9):1–27. doi: 10.3390/s21093191.
[33] Mayer KM, Hafner JH. Localized surface plasmon resonance sensors. Chem Rev. 2011;111(6):3828–57. doi: 10.1021/cr100313v.
[34] Endo T, Yamamura S, Nagatani N, Morita Y, Takamura Y, Tamiya E. Localized surface plasmon resonance based optical biosensor using surface modified nanoparticle layer for label-free monitoring of antigen–antibody reaction. Sci Technol Adv Mat. 2005;6(5):491–500. doi: 10.1016/j.stam.2005.03.019.
[35] Endo T, Kerman K, Nagatani N, Takamura Y, Tamiya E. Label-free detection of peptide nucleic acid−DNA hybridization using localized surface plasmon resonance based optical biosensor. Anal Chem. 2005;77(21):6976–84. doi: 10.1021/ac0513459.
[36] Endo T, Kerman K, Nagatani N, Hiepa HM, Kim DK, Yonezawa Y, et al. Multiple label-free detection of antigen−antibody reaction using localized surface plasmon resonance-based core−shell structured nanoparticle layer nanochip. Anal Chem. 2006;78(18):6465–75. doi: 10.1021/ac0608321.
[37] Endo T, Kerman K, Nagatani N, Tamiya E. Excitation of localized surface plasmon resonance using a core–shell structured nanoparticle layer substrate and its application for label-free detection of biomolecular interactions. J Phys Condens Mat. 2007;19(21):1–10. doi: 10.1088/0953-8984/19/21/215201.
[38] Hiep HM, Endo T, Kerman K, Chikae M, Kim DK, Yamamura S, et al. A localized surface plasmon resonance based immunosensor for the detection of casein in milk. Sci Technol Adv Mat. 2007;8(4):331–8. doi: 10.1016/j.stam.2006.12.010.
[39] Wang L, Zhu H, Hou H, Zhang Z, Xiao X, Song Y. A novel hydrogen peroxide sensor based on Ag nanoparticles electrodeposited on chitosan-graphene oxide/cysteamine-modified gold electrode. J Solid State Electr. 2012;16(4):1693–700. doi: 10.1007/s10008-011-1576-4.
[40] Endo T, Yanagida Y, Hatsuzawa T. Quantitative determination of hydrogen peroxide using polymer coated Ag nanoparticles. Measurement. 2008;41(9):1045–53. doi: 10.1016/j.measurement.2008.03.004.
[41] Alzahrani E. Colorimetric detection based on localised surface plasmon resonance optical characteristics for the detection of hydrogen peroxide using acacia gum–stabilised silver nanoparticles. Anal Chem Insights. 2017;12:1–10. doi: 10.1177/1177390116684686.
[42] Filippo E, Serra A, Manno D. Poly(vinyl alcohol) capped silver nanoparticles as localized surface plasmon resonance-based hydrogen peroxide sensor. Sensor Actuat B Chem. 2009;138(2):625–30. doi: 10.1016/j.snb.2009.02.056
[43] Marinescu L, Ficai D, Oprea O, Marin A, Ficai A, Andronescu E, et al. Optimized synthesis approaches of metal nanoparticles with antimicrobial applications. J Nanomater. 2020;2020:1–14. doi: 10.1155/2020/6651207.
[44] Spina RL, Mehn D, Fumagalli F, Holland M, Reniero F, Rossi F, et al. Synthesis of citrate-stabilized silver nanoparticles modified by thermal and pH preconditioned tannic acid. Nanomaterials. 2020;10(10):1–16. doi: 10.3390/nano10102031.
[45] Pascu B, Negrea A, Ciopec M, Duteanu N, Negrea P, Bumm LA, et al. Silver nanoparticle synthesis via photochemical reduction with

sodium citrate. Int J Mol Sci. 2023;24(1):1–17. doi: 10.3390/ijms24010255.

[46] Medina-Ramirez I, Bashir S, Luo Z, Liu JL. Green synthesis and characterization of polymer-stabilized silver nanoparticles. Colloid Surface B. 2009;73(2):185–91. doi: 10.1016/j.colsurfb.2009.05.015.

[47] Putri GE, Gusti FR, Sary AN, Zainul R. Synthesis of silver nanoparticles used chemical reduction method by glucose as reducing agent. J Phys Conf Ser. 2019;1317:1–8. doi: 10.1088/1742-6596/1317/1/012027.

[48] Raveendran P, Fu J, Wallen SL. Completely "Green" synthesis and stabilization of metal nanoparticles. J Am Chem Soc. 2003;125(46):13940–1. doi: 10.1021/ja029267j.

[49] Ayala G, Vercik LCO, Menezes TAV, Vercik A. A simple and green method for synthesis of Ag and Au nanoparticles using biopolymers and sugars as reducing agent. Mater Res Soc Symp P. 2012;1386:1–7. doi: 10.1557/opl.2012.645.

[50] Chen Q, Liu G, Chen G, Mi T, Tai J. Green synthesis of silver nanoparticles with glucose for conductivity enhancement of conductive ink. Bioresources. 2016;12(1):608–21. doi: 10.15376/biores.12.1.608-621.

[51] Handoko CT, Huda A, Bustan MD, Yudono B, Gulo F. Green synthesis of silver nanoparticle and its antibacterial activity. Rasayan J Chem. 2017;10(4):1137–44. doi: 10.7324/RJC.2017.1041875.

[52] Tyagi PK, Tyagi S, Gola D, Arya A, Ayatollahi SA, Alshehri MM, et al. Ascorbic acid and polyphenols mediated green synthesis of silver nanoparticles from Tagetes erecta L. aqueous leaf extract and studied their antioxidant properties. J Nanomater. 2021;2021:1–9. doi: 10.1155/2021/6515419.

[53] Chelly M, Chelly S, Zribi R, Bouaziz-Ketata H, Gdoura R, Lavanya N, et al. Synthesis of silver and gold nanoparticles from Rumex roseus plant extract and their application in electrochemical sensors. Nanomaterials. 2021;11(3):1–17. doi: 10.3390/nano11030739.

[54] Peng C, Duan X, Xie Z, Liu C. Shape-controlled generation of gold nanoparticles assisted by dual-molecules: The development of hydrogen peroxide and oxidase-based biosensors. J Nanomater. 2014;2014:1–7. doi: 10.1155/2014/576082.

[55] Srikhao N, Ounkaew A, Kasemsiri P, Theerakulpisut S, Okhawilai M, Hiziroglu S. Green synthesis of silver nanoparticles using the extract of spent coffee used for paper-based hydrogen peroxide sensing device. Sci Rep. 2022;12(1):1–12. doi: 10.1038/s41598-022-22067-6.

[56] Al-Ansari MM, Al-Dahmash ND, Ranjitsingh AJA. Synthesis of silver nanoparticles using gum Arabic: Evaluation of its inhibitory action on Streptococcus mutans causing dental caries and endocarditis. J Infect Public Heal. 2021;14(3):324–30. doi: 10.1016/j.jiph.2020.12.016.

[57] Khan N, Kumar D, Kumar P. Silver nanoparticles embedded guar gum/gelatin nanocomposite: Green synthesis, characterization and antibacterial activity. Colloid Interface Sci Commun. 2020;35:1–7. doi: 10.1016/j.colcom.2020.100242.

[58] Ravindran RSE, Subha V, Ilangovan R. Silver nanoparticles blended PEG/PVA nanocomposites synthesis and characterization for food packaging. Arab J Chem. 2020;13(7):6056–60. doi: 10.1016/j.arabjc.2020.05.005.

[59] El-Sheikh MA, El-Rafie SM, Abdel-Halim ES, El-Rafie MH. Green synthesis of hydroxyethyl cellulose-stabilized silver nanoparticles. J Polym. 2013;2013(1):1–11. doi: 10.1155/2013/650837.

[60] Mehata MS. Green route synthesis of silver nanoparticles using plants/ginger extracts with enhanced surface plasmon resonance and degradation of textile dye. Mater Sci Eng B. 2021;273:1–9. doi: 10.1016/j.mseb.2021.115418.

[61] Ghaseminezhad SM, Hamedi S, Shojaosadati SA. Green synthesis of silver nanoparticles by a novel method: Comparative study of their properties. Carbohyd Polym. 2012;89(2):467–72. doi: 10.1016/j.carbpol.2012.03.030.

[62] Mouzaki M, Maroui I, Mir Y, Lemkhente Z, Attaoui H, Ouardy KE, et al. Green synthesis of silver nanoparticles and their antibacterial activities. Green Process Synth. 2022;11(1):1136–47. doi: 10.1515/gps-2022-0061.

[63] Pongsamart S, Panmaung T. Isolation of polysaccharides from fruit-hulls of durian (Durio zibethinus L.). Warasan Songkhla Nakharin. 1998;20(3):323–32.

[64] Tagad CK, Dugasani SR, Aiyer R, Park S, Kulkarni A, Sabharwal S. Green synthesis of silver nanoparticles and their application for the development of optical fiber based hydrogen peroxide sensor. Sensor Actuat B Chem. 2013;183:144–9. doi: 10.1016/j.snb.2013.03.106.

[65] Nitinaivinij K, Parnklang T, Thammacharoen C, Ekgasit S, Wongravee K. Colorimetric determination of hydrogen peroxide by morphological decomposition of silver nanoprisms coupled with chromaticity analysis. Anal Methods. 2014;6(24):9816–24. doi: 10.1039/C4AY02339K.

[66] Zhang L, Li L. Colorimetric detection of hydrogen peroxide using silver nanoparticles with three different morphologies. Anal Methods. 2016;8(37):6691–5. doi: 10.1039/C6AY01108J.

[67] Hokputsa S, Gerddit W, Pongsamart S, Inngjerdingen K, Heinze T, Koschella A, et al. Water-soluble polysaccharides with pharmaceutical importance from durian rinds (Durio zibethinus Murr.): isolation, fractionation, characterisation and bioactivity. Carbohyd Polym. 2004;56(4):471–81. doi: 10.1016/j.carbpol.2004.03.018.

[68] Farrokhnia M, Karimi S, Momeni S, Khalililaghab S. Colorimetric sensor assay for detection of hydrogen peroxide using green synthesis of silver chloride nanoparticles: Experimental and theoretical evidence. Sensor Actuat B Chem. 2017;246(C):979–87. doi: 10.1016/j.snb.2017.02.066.